Biomimetic Assembly of Polypeptide-Stabilized $CaCO_3$ Nanoparticles

Zhongping Zhang,*,† Daming Gao,† Hui Zhao,† Chenggen Xie,† Guijian Guan,† Dapeng Wang,† and Shu-Hong Yu*,‡

Institute of Intelligent Machines, Chinese Academy of Sciences, Hefei, Anhui 230031, P.R. China, and Hefei National Laboratory for Physical Science at Microscale, School of Chemistry & Materials, University of Science and Technology of China, Hefei, Anhui 230026, P.R. China

Received: February 9, 2006; In Final Form: March 14, 2006

In this paper, we report a simple polypeptide-directed strategy for fabricating large spherical assembly of $CaCO_3$ nanoparticles. Stepwise growth and assembly of a large number of nanoparticles have been observed, from the formation of an amorphous liquidlike $CaCO_3$-polypeptide precursor, to the crystallization and stabilization of polypeptide-capped nanoparticles, and eventually, the spherical assembly of nanoparticles. The "soft" poly(aspartate)-capping layer binding on a nanoparticle surface resulted in the unusual soft nature of nanoparticle assembly, providing a reservoir of primary nanoparticles with a moderate mobility, which is the basis of a new strategy for reconstructing nanoparticle assembly into complex nanoparticle architectures. Moreover, the findings of the secondary assembly of nanoparticle microspheres and the morphology transformation of nanoparticle assembly demonstrate a flexible and controllable pathway for manipulating the shapes and structures of nanoparticle assembly. In addition, the combination of the polypeptide with a double hydrophilic block copolymer (DHBC) allows it to possibly further control the shape and complexity of the nanoparticle assembly. A clear perspective is shown here that more complex nanoparticle materials could be created by using "soft" biological proteins or peptides as a mediating template at the organic−inorganic interface.

Introduction

The assembly of nanoparticles has recently attracted extensive interest due to its importance in the application of particle-based materials. Surface-stabilized nanoparticles, as nanoscale building blocks, can spontaneously assemble into various morphologically controlled or highly ordered nanostructures, which is usually manipulated by tailoring the surface properties of nanoparticles by using organic capping layers or chemically installing functionality on nanoparticle surfaces through organic synthesis.[1−10] In the absence of a sufficiently strong surface-protecting layer, however, it seems that nanoparticles would always randomly aggregate into disordered condensed solids. It has been well established that organic ligands with high nanoparticle binding affinities can promote self-assembly, driven by the interactions between surface-absorbed ligands. Several assembly strategies have recently been explored by using layer-by-layer assembling,[7] molecular cross-linking,[8−10] microbial/virus templating,[11−13] and polymer-based recognition.[4,14] While various assembled nanostructures have been made, the ability to precisely control assembly size, morphology, and structure is still a challenge.

In biological systems, however, the finely tuned morphologies or architectures of naturally occurring materials can be precisely directed by organized biomacromolecules, in which self-assembly is one of the main driving forces for constructing complex biological structures.[15−17] The bioinspired strategies, on the basis of biological concepts and mechanisms, have been developed and widely applied to synthesize and assemble elaborate nanoarchitectures.[15,18−20] Among various biomimetic assembly approaches aimed for constructing nanostructures, employing biopolymers as assembly components may provide predictable recognition and considerable flexibility due to their high selectivity and self-organization ability. Well-defined nanostructures have been successfully assembled with oligonucleotide−oligonucleotide pairing,[21] peptide−peptide recognizing,[22] streptavidin/biotin binding,[23] and antibody/antibody matching.[24] It has also been demonstrated that the simplest model molecule of peptide (formamide, containing a prototype amide HNC═O peptide linkage[25]) can drive the 3D oriented aggregation of nanoparticles into monocrystalline architectures, and the self-organization of 3D dendritic nanoarchitectures.[26]

In this paper, we report a biomimetic self-assembly of calcium carbonate nanoparticles directed by long-chain polypeptide. About half a million of the 15−25 nm vaterite nanoparticles can be assembled into highly spherical aggregates through a stepwise process from amorphous liquidlike $CaCO_3$-polypeptide precursor to the crystallization and stabilization of polypeptide-capped vaterite nanoparticles, and eventually, the spherical assembly of nanoparticles. The soft nature of the assembled microsphere has clearly been demonstrated by the partial spreading of nanoparticles on a wafer substrate and thorough disbanding of microspheres under ultrasonication treatment. The "soft" polypeptide chains binding onto the nanoparticle surface provide the nanoparticles with a moderate mobility, which allows for reconstructing the morphologies and structures of nanoparticle assembly. For example, the nanoparticle microspheres could further assemble into larger spherical aggregates, and undergo reconstructing to form larger nanoparticle spheres with dense internal texture. Furthermore, more complex as-

* Address correspondence to this author. E-mail: zpzhang@iim.ac.cn; shyu@ustc.edu.cn.

† Institute of Intelligent Machines, Chinese Academy of Sciences.

‡ Hefei National Laboratory for Physical Science at Microscale, School of Chemistry & Materials, University of Science and Technology of China.

10.1021/jp060838u CCC: $33.50
Published on Web 04/07/2006

semblies such as peanut-like nanoparticle architectures can also be fabricated from the polypeptide-capped nanoparticles when the templating force was exerted by a double hydrophibic block copolymer (DHBC).

Experimental Section

Chemicals and Materials. Analytic grade poly(aspartic acid) sodium (M_w = 14 900, Sigma), calcium chloride ($CaCl_2 \cdot 2H_2O$, 99.99%, Aldrich), and ammonium carbonate (99.99%, Aldrich) were used without further purification. Poly(ethylene oxide)-*block*-poly(methacrylic acid) (PEO-*b*-PMAA, PEO = 3000 g/mol, PMAA = 700 g/mol) is a commercial product from The Goldschmidt AG. All glassware and small pieces of silicon wafer substrate were soaked in a mixing H_2SO_4/H_2O_2 solution (7:3, v/v), then rinsed with doubly distilled water, and finally dried under nitrogen airflow.

Experimental Procedures. Poly(aspartic acid) sodium and calcium chloride were dissolved in 50 mL of boiled deionized water under vigorous stirring to make an aqueous solution containing 1 mg/mL of poly(aspartic acid) sodium and 0.01 M $CaCl_2$. The synthesis and assembly of vaterite nanoparticles were carried out in a closed desiccator through a $(NH_4)_2CO_3$ vapor diffusion procedure at room temperature as described previously.[27] The glass vial containing 10 mL of the mixture stock solution was covered with Parafilm, which was then punched with three needle holes and placed in a desiccator. At the same time, a small bottle of $(NH_4)_2CO_3$ powder was also covered with Parafilm punched with three needle holes and placed on the bottom of the desiccator. After different periods of time, the product was separated by centrifugation, washed with alcohol, and then dried at room temperature. Meanwhile, a similar synthesis procedure was also used to prepare the peanut-like assembly of nanoparticles with addition of PEO-*b*-PMAA.

To test the soft−hard nature of the as-synthesized nanoparticle microspheres, a drop of diluted particle solution was cast onto the surface of a cleaning wafer substrate, then dried at room temperature naturally. The particles deposited on the wafer substrate were gently removed onto a piece of copper foil. Then the contacting area of microspheres with wafer substrate was examined with a scanning electron microscope (SEM).

Characterization. The X-ray diffraction pattern of vaterite particles was recorded with a Bruker AXS GADDS X-ray diffractometer. The morphology of nanoparticle assembly was observed by means of a JEOL JSM-6700 field-emission scanning electron microscope (FE-SEM). The primary nanoparticles were analyzed with use of a JEOL 3010 transmission electron microscope. Attenuated total reflection infrared analysis was carried out on a PerkinElmer FT-IR spectrometer equipped with a liquid nitrogen cooled narrow-banded mercury cadmium telluride detector.

Results and Discussion

Calcium carbonate has been of considerable interest because it is widely used as a model system for studying the biomimetic process due to its abundance in nature. A key principle in biomineralization is the involvement of biological macromolecules, such as phosphoproteins and glycoproteins that have high binding affinity to the surface of $CaCO_3$ crystallites so as to achieve growth control in size, shape, and structure.[15] The acidic amide acids, such as aspartic acid and glutamic acid, are the primary active units of the mineralization proteins on the organic/inorganic interface of biomineralized tissues.[28] Here, we thus chose the synthesized poly(aspartic acid) sodium with a relatively large molecular weight (M_w = 14 900) to guide the self-assembly of $CaCO_3$ nanoparticles. The synthesis and assembly of nanoparticles are coupled in situ to produce nanoparticle ensembles in aqueous media through vapor diffusion of $(NH_4)_2CO_3$. The structure and composition of as-synthesized sample confirmed by powder XRD diffraction is hexagonal $CaCO_3$ vaterite with phase purity, as shown in Figure 1A. The obvious broadening of XRD diffraction lines indicates that nanoparticles are very small. The particle size determined from the X-ray diffraction data with the Debye−Scherrer formula is about 20 nm. The particle suspension was stable for two weeks without noticeable precipitation. However, the product could be isolated easily by centrifugation at a low speed, suggesting the presence of large $CaCO_3$ particles. After 2 days, the product was isolated from solution and examined by scanning electron microscopy (SEM). We found that the product is large $CaCO_3$ microspheres instead of small nanoparticles, as revealed by the low-magnification SEM image of Figure 1B. The microsphere size ranges from 1 to 2 μm. Interestingly, the high-magnification SEM image in Figure 1C shows a highly spherical assembly of primary nanoparticles, which is built up of small nanoparticles with a size of 15−25 nm. Thus, each microsphere with a size of 1−2 μm consists of about half a million 15−25 nm vaterite nanoparticles. Furthermore, the uniform nanoparticle feature of internal texture is also revealed by the cross-section observation of the microsphere, as shown in the SEM image of Figure 1D. The average size of primary nanoparticles is in good agreement with the calculated value from X-ray diffraction data, indicating that the XRD line broadening results from the small size of primary particles in the large spherical assembly. Analogous biogenic ZnS nanoparticle microspheres and microemulsion-templated Au nanoparticle spheres have been reported recently.[29,30]

Meanwhile, the nanoparticle microspheres reported here possess interesting structures and properties, different from both the common hard−solid aggregates by interparticle fusion connection[31] and very soft spongelike assembly by interparticle covalent linker.[8] Although the present nanoparticle assembly is stable in solution, a slight conglutination between microspheres could occur when centrifugation separation was completed (Figure 1B). Detailed observation suggests that the periphery between adhesive microspheres is not perfectly spherical as indicated with the arrows in Figure 1B, implying that the spherical assembly was likely soft. To confirm further the soft nature of assembly, a drop of freshly prepared particle solution was dried on a piece of wafer substrate at room temperature. SEM observation shows that the contacting area of the microsphere with the substrate surface becomes very flat as indicated with arrows in the SEM image of Figure 2A. The primary nanoparticles on the contacting surface are closely arranged in a planar fashion, and display a tendency to slightly spread on the substrate surface (Figure 2B). These confirm clearly that the assembly has a relatively soft nature to allow the mobility of nanoparticles for their rearrangement. As an additional piece of evidence to directly support the assembly nature, ultrasonic treatment was applied to test the viability of breaking the interparticle linkage. It was found that the spherical assembly was disbanded thoroughly into discrete nanoparticles under ultrasonication in alcohol, as shown in the TEM image of Figure 2C. The selective area electron diffraction (SAED) was also indexed to the polycrystalline circles of primary vaterite nanoparticles with phase purity (inset ED pattern in Figure 2C). Therefore, the facts that the assembly has a soft nature and can be disbanded demonstrate the nature of a novel and distinct spherical assembly.

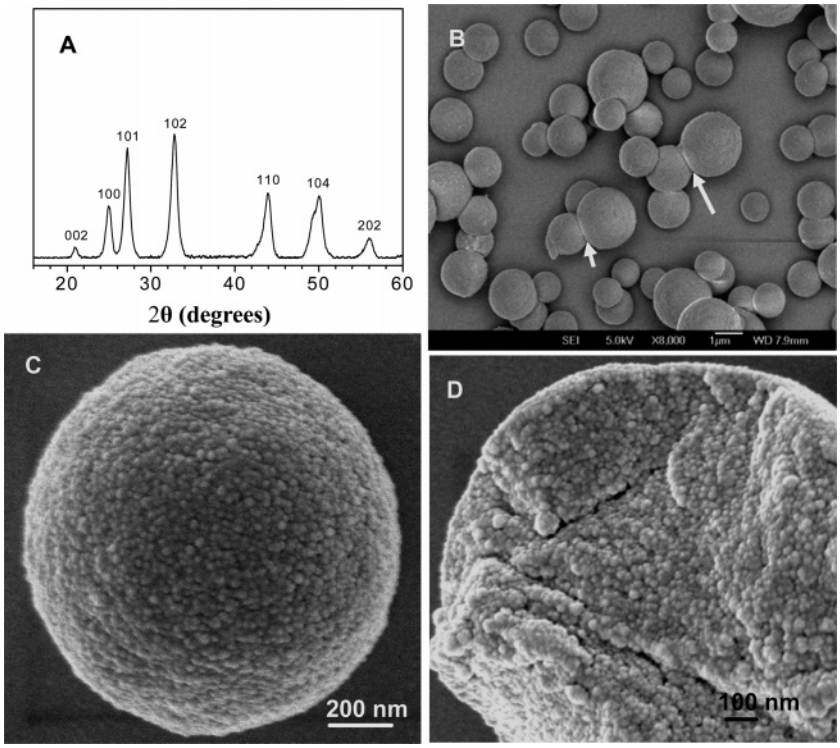

Figure 1. (A) The powder XRD pattern and (B) SEM micrographs of as-synthesized $CaCO_3$ microspheres after 2 days of growth period. (C) A high-magnification SEM image showing that an individual microsphere consists of numerous small nanoparticles ~15−25 nm in size. (D) A cross-section SEM image revealing the internal nanoparticle texture of microspheres.

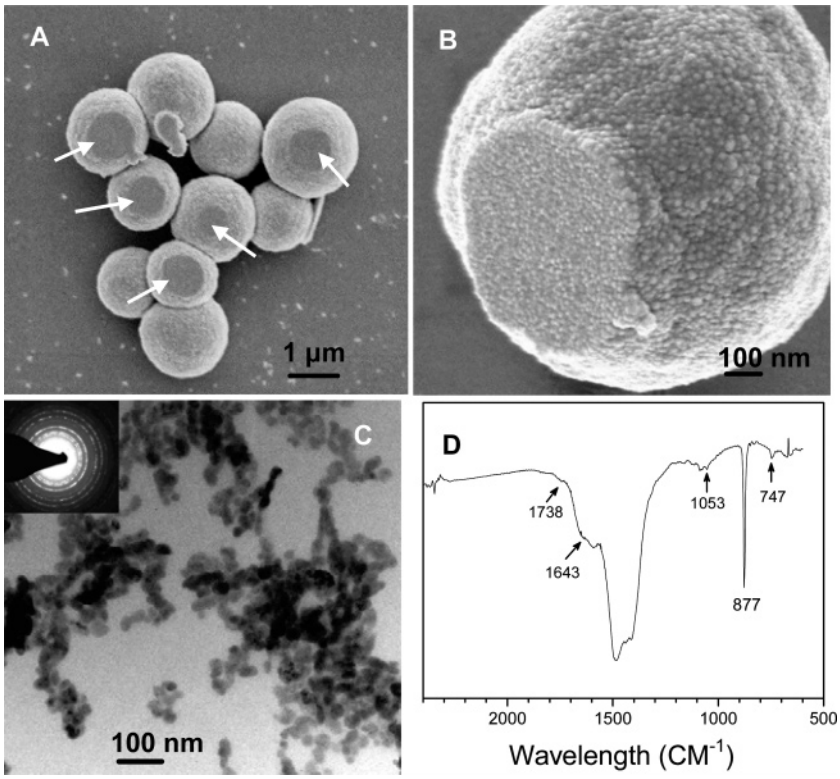

Figure 2. (A−C) SEM and TEM micrographs showing the soft nature and redispersing ability of vaterite nanoparticle microspheres: (A) SEM image of the contacting area of microspheres with wafer substrate surface, (B) high-magnification SEM images of the surface-contact area, and (C) TEM image of primary nanoparticles redispersed from microspheres with ultrasonication (inset is the SAED image). (D) Attenuated total reflection (ATR) infrared spectroscopy of the redispersive primary nanoparticles.

To obtain a better understanding of the assembly mechanism, the attenuated total reflection (ATR) infrared spectroscopy of the redispersed nanoparticles was measured to assess the interaction between polypeptide molecules and nanoparticles. Figure 2D shows the ATR-FTIR spectra of primary nanoparticles obtained by ultrasonic treatment in alcohol. In addition to characteristic bands of the vaterite polymorph at 877 and 747 cm^{-1},[32] the infrared data display clearly the CONH band at 1643 cm^{-1} and the carboxyl group band at 1738 cm^{-1}, and the stretching band of the peptide backbone at 1053 cm^{-1}.[33]

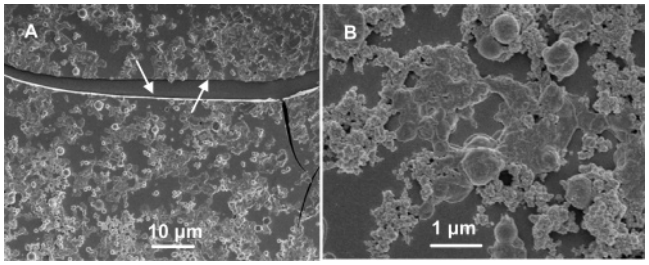

Figure 3. A stepwise process from an amorphous liquidlike precursor to vaterite crystalline transition at the early stage of mineralization: (A) SEM image of the film formed by drying a droplet of reaction solution on a glass substrate after a 2 h mineralizing period and (B) SEM image of the vaterite nanoparticles and small aggregates formed after a 12 h mineralizing period.

These results confirm that poly(aspartic acid) molecules remain attached to the nanoparticle surface in the separated samples. A soft coating layer of poly(aspartate) may form by complexation of acidic carboxyl groups to the surface calcium ions of nanoparticles. On the other hand, it is well-known that vaterite is thermodynamically unstable and can transform easily into stable calcite by the Ostwald ripening process. The solvent-mediated transformation from vaterite into calcite should occur extremely rapidly for the small vaterite particle ~20 nm in size. In our case, therefore, the high stabilization and self-assembly of vaterite nanoparticles is an additional piece of direct evidence for the formation of polypeptide shells because the phase transformation is blocked completely, as confirmed by the XRD pattern and the selected area electron diffraction (SAED) pattern. Moreover, the polypeptide shells greatly inhibited the fusion connection of nanoparticles themselves, which usually occurs in the vaterite particle aggregates with use of simple aspartic acids as organic ligands.[31]

To explore further the growth and assembly mechanism of vaterite nanoparticles, we examined the intermediate products at different stages with a scanning electron microscope (Figure 3). At an early stage of mineralization (after reaction for 2 h), an amorphous liquidlike precursor was observed, which typically occurs in a mineralization system containing polypeptide.[34] When a drop of reaction solution was dried on a glass slide, a layer of amorphous film with a uniform thickness was formed on the substrate surface (as indicated by arrows in the SEM image of Figure 3A). This suggests clearly a polymer-induced liquid-precursor process as reported by Gower et al.[34] After a critical induction time, the poly(aspartate) could further induce the vaterite nucleation from amorphous $CaCO_3$-polypeptide precursor, and the subsequent crystalline growth of nanoparticles. Meanwhile, some primary nanoparticles began to stick together loosely or form small spherical aggregates after 12 h (Figure 3B). Here, poly(aspartate) molecules appear to play a crucial role in controlling the formation and assembly of nanoparticles. The long-chain peptide inhibited the vaterite nanoparticle from thermodynamically transforming into calcite by binding onto the surface of the growing nanocrystallites. Moreover, the adsorption of poly(aspartate) at high surface concentration on the nanoparticle surface results in a vaterite−polypeptide gel,[34b] which may also inhibit further crystallization growth of vaterite nanoparticles. That is to say, the polypeptide molecule layer can terminate the growth of nanoparticles and stabilize those vaterite nanoparticles. As illustrated in Figure 4, the above results demonstrate a three-step process to form large microspheres in the present reaction system: the formation of amorphous $CaCO_3$-polypeptide precursor, the growth of polypeptide-capped nanoparticles, and subsequent assembly of

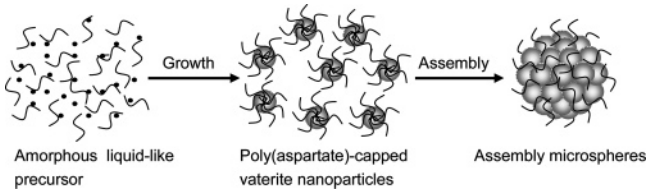

Figure 4. Schematic illustration of a three-step process for the formation of vaterite nanoparticle microspheres.

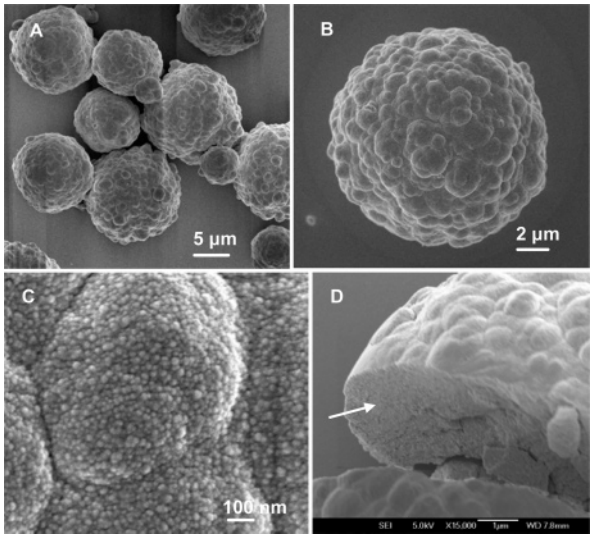

Figure 5. SEM micrographs showing the microsphere aggregates assembled from numerous 1−2 μm microspheres after staying in assembly solution for one week: (A) overview SEM image, (B) SEM image of a single microsphere aggregate, (C) high-magnification SEM image, and (D) inside-view SEM image.

nanoparticles. Generally, van der Waals force is believed to drive the aggregate growth of nanostructures in biomimetic mineralization. In our case, however, the interaction between polypeptide chains such as hydrogen bonds may be one of the main driving forces for the nanoparticle assembly because of the "soft" poly(aspartate)-capping layer binding on the surface of nanoparticles.

In addition to the soft nature, further experiments revealed that vaterite nanoparticles in microspheres are kept slightly apart by the polypeptide-capped layer, to allow for their reconstruction or reorganization. When the microspheres stayed in the assembly solution for one week, they could further assemble into larger spherical aggregates ~10−15 μm in size, as shown in Figure 5A. The primary nanoparticles as well as the boundary between microspheres can clearly be recognized from the surface view by low- and high-magnification SEM (Figure 5B,C). In the interior of secondary spheres, however, the boundaries and voids between microspheres disappeared completely, and the primary nanoparticles emerged together completely to form a dense nanoparticle texture, as indicated with the arrow in the SEM image of Figure 5D. In fact, some smaller aggregates consisting of several microspheres as intermediate product were also observed in our experiment (SEM images not shown). These observations suggest a hierarchical assembly process as illustrated in Figure 6. First, numerous 1−2 μm microspheres tend to aggregate into a larger sphere in assembly solution due to the interaction of polypeptide molecules on the surface of those microspheres. Then, primary nanoparticles in different microspheres undergo restructuring or rearranging into a more compact/dense nanoparticle texture, resulting in the disappearance of boundaries and voids between microspheres, as shown in Figure 5D. Such a reconstructing process is rarely demon-

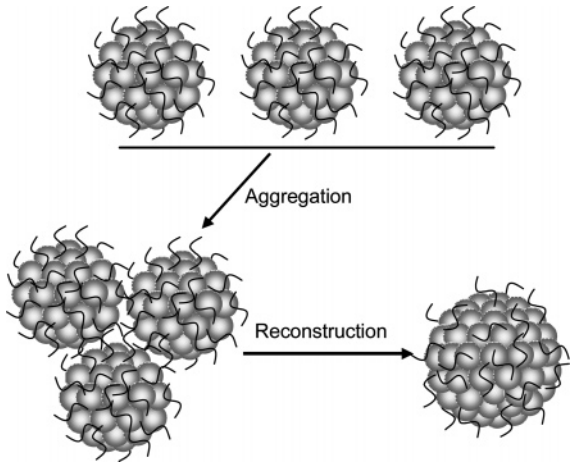

Figure 6. Schematic illustration of the secondary assembly process through aggregation and reconstruction from nanoparticle microspheres into larger nanoparticle spheres.

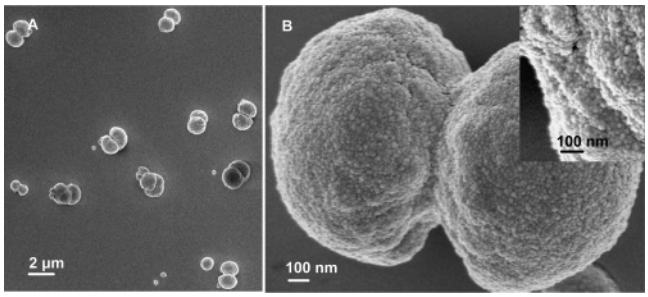

Figure 7. Unusual peanut-like assembly of polypeptide-shell-stabilized nanoparticles with addition of PEO-*b*-PMAA molecules: (A) overview SEM image and (B) high-magnification SEM images (inset is the SEM image of a broken peanut-like particle).

strated by experimental observation in previous research on nanoparticle assembly or biomimetic mineralization. Usually, regular self-assembly requires that aggregated particles can equilibrate with nonaggregated ones in solution and adjust their position relative to one another in an aggregate. The "soft" polypeptide shells keep nanoparticles slightly apart, and may provide the primary nanoparticles with a moderate mobility ability for regulating their position in an aggregate, which is typically thought to occur in the process of oriented attachment of biomineralization.[35]

Usually, spherical aggregation is energetically favored because the formation of microspheres can greatly reduce the interfacial energy of primary nanoparticles. However, the moderate mobility of interparticles resulting from the stabilization ability of the poly(aspartate)-capping layer offers the possibility to fabricate more complex nanoparticle structures, which forms the basis of a new strategy for reconstructing nanoparticle assembly into more complex architectures. Recently, a so-called double hydrophibic block copolymer (DHBC) has been frequently used to produce the complex hierarchical nanostructures of mineral materials,[36] we thus chose PEO-*b*-PMAA as macromolecule templates to further modulate the assembly behavior of nanoparticles together with poly(aspartate). An obvious geometric effect on the assembly morphology of polypeptide-capped nanoparticles was demonstrated when the templating force was exerted by PEO-*b*-PMAA molecules. Figure 7A shows that the peanut-like microparticles instead of spherical ones were produced in the assembly solution, which indicates a strong modification on assembly morphology. The resulting peanut-like assembly is also built up of numerous small nanoparticles with the same particle size of 15∼25 nm (Figure 7B). The SEM image of a broken particle in the inset of Figure 7B further confirms that the peanut-like microparticles consist entirely of dense primary nanoparticles. Even though the peanut-like crystalline particles have been grown by various approaches of biomimetic synthetic and colloidal chemistry,[37] the vaterite peanut-like assemblies composed of primary nanoparticles in the present case have been rarely observed.

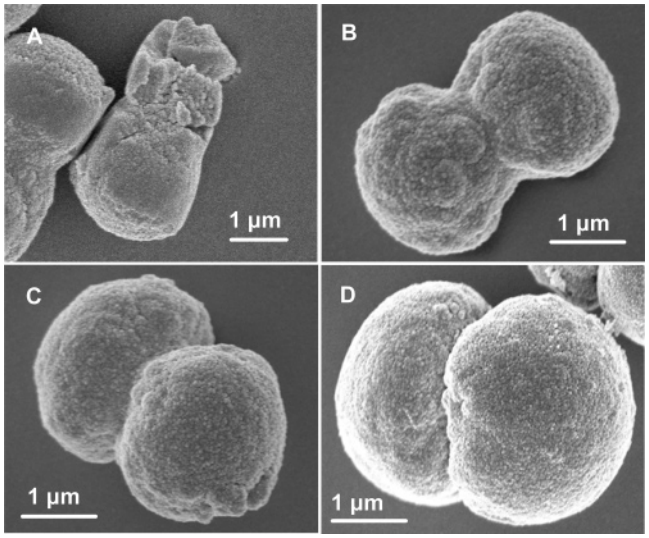

Figure 8. Progressive self-assembly process of primary nanoparticles from rodlike particles (A) through dumbbell-like secondary particles (B and C) into nearly closed spheres (D).

Furthermore, morphology evolution of the peanut-like assembly at different growth stage was monitored. A progressive self-assembly process of primary nanoparticles was observed from rodlike particles through peanut/dumbbell-like secondary particles into the nearly closed spheres (Figure 8), sharing the same scenario as reported previously.[37e,f] The morphology evolution suggests further that peanut-like assembly resulted from the progressive aggregation of primary nanoparticles driven by both the templating force of PEO-*b*-PMAA molecules and interaction of polypeptide shells. Although the formation mechanism of peanut-like assembly has yet to be understood, the ability to perform such assembly transformation holds the promise for creating more complex nanostructured materials with use of "soft" biological proteins or peptides.

In conclusion, we have developed a simple polypeptide-directed strategy for large spherical assembly of $CaCO_3$ nanoparticles without the use of complex templates such as emulsions and polymer scaffold beads. Stepwise growth and assembly of a large number of nanoparticles have been observed, from the formation of an amorphous liquidlike $CaCO_3$-polypeptide precursor, to the crystallization and stabilization of polypeptide-capped vaterite nanoparticles, and, eventually, the spherical assembly of nanoparticles. The unusual soft nature of nanoparticle assembly due to the poly(aspartate)-capping layer was clearly revealed, and provides primary nanoparticles with a moderate mobility, which is the basis of a new strategy for reconstructing nanoparticle assembly into complex nanoparticle architectures. The addition of a double hydrophilic block copolymer (DHBC) in the present mineralization system can further control the shape and complexity of the nanoparticle assembly. Furthermore, the findings of the secondary assembly of microspheres and the morphology transformation of nanoparticle assembly demonstrate a flexible and controllable pathway for manipulating the shapes and structures of nanoparticle assembly. The reported results here may be helpful in

understanding the self-assembly mechanism of complex organic−inorganic hybrid materials in the biomineralization process.

Acknowledgment. We genuinely thank Prof. Dr. H. Cölfen and Prof. Dr. M. Antonietti for donating the double hydrophilic block copolymers we used in this study. This work was supported by the National Natural Science Foundation of China (No. 60571038) and the National Basic Research Program of China (2006CB300407). We also are thankful for the financial support from the Centurial Program of the Chinese Academy of Sciences, the Natural Science Foundation of China (Nos. 20325104, 20321101, 50372065), and the Scientific Research Foundation for the Returned Overseas Chinese Scholars supported by the State Education Ministry.

References and Notes

(1) Whitesides, G. M.; Grzybowski, B. *Science* **2002**, *295*, 2418.
(2) Wang, Z. L. *Adv. Mater.* **1998**, *10*, 13.
(3) van Bommel, K. J. C.; Friggeri, A.; Shinkai, S. *Angew. Chem., Int. Ed.* **2003**, *42*, 980.
(4) Shenhar, R.; Norsten, T. B.; Rotello, V. M. *Adv. Mater.* **2005**, *17*, 657.
(5) Li, M.; Schnablegger, H.; Mann, S. *Nature* **1999**, *402*, 393.
(6) Fan, H.; Chen, Z.; Brinker, C. J.; Clawson, J.; Alam, T. *J. Am. Chem. Soc.* **2005**, *127*, 13746.
(7) Shipway, A. N.; Lahav, M.; Blonder, R.; Willner, I. *Chem. Mater.* **1999**, *11*, 13.
(8) Maye, M. M.; Lim, I. S.; Luo, J.; Rab, Z.; Rabinovich, D.; Liu, T.; Zhong, C. J. *J. Am. Chem. Soc.* **2005**, *127*, 1519.
(9) Yang, P.; Zhao, D.; Margolese, D. I.; Chmelka, B. F.; Stucky, G. D. *Nature* **1998**, *396*, 125.
(10) Butler, R.; Davies, C. M.; Cooper, A. I. *Adv. Mater.* **2001**, *13*, 1459.
(11) Chan, C. S.; Stasio, G. D.; Welch, S. A.; Girasole, M.; Frazer, B. H.; Nesterova, M. V.; Fakra, S.; Banfield, J. F. *Science* **2004**, *303*, 1656.
(12) Flynn, C. E.; Lee, S. W.; Peelle, B. R.; Belcher, A. M. *Acta Mater.* **2003**, *51*, 5867.
(13) Dujardin, E.; Peet, C.; Stubbs, G.; Culver, J. N.; Mann, S. *Nano Lett.* **2003**, *3*, 413.
(14) Schmid, G.; Baumle, M.; Beyer, N. *Angew. Chem., Int. Ed.* **2000**, *39*, 181.
(15) (a) Mann, S. *Biomineralization*: *Principles and Concepts in Bioinorganic Materials Chemistry*; Oxford University Press: New York, 2001. (b) Lowenstam, H. A.; Weiner, S. *On Biomineralization*; Oxford University Press: Oxford, UK, 1989.
(16) Aizenberg, J.; Tkachenko, A.; Weiner, S.; Addadi, L.; Hendler, G. *Nature* **2001**, *412*, 819.
(17) Su, X.; Belcher, A. M.; Zaremba, C. M.; Morse, D. E.; Stucky, G. D.; Heuer, A. H. *Chem. Mater.* **2002**, *14*, 3106.
(18) (a) Cölfen, H.; Mann, S. *Angew. Chem., Int. Ed.* **2003**, *42*, 2350. (b) Mann, S. *Angew. Chem., Int. Ed.* **2000**, *39*, 3392. (c) Cölfen, H.; Yu, S. H. *MRS Bull.* **2005**, *30*, 727. (d) Naka, K. *Top. Curr. Chem.* **2003**, *228*, 141.
(19) (a) Estroff, L. A.; Hamilton, A. D. *Chem. Mater.* **2001**, *13*, 3227.
(20) (a) Naka, K.; Chujo, Y. *Chem. Mater.* **2001**, *13*, 3245. (b) Kato, T.; Sugawara, A.; Hosoda, N. *Adv. Mater.* **2002**, *14*, 869.
(21) (a) Storhoff, J. J.; Mirkin, C. A. *Chem. Rev.* **1999**, *99*, 1849. (b) Mirkin, C. A.; Letsinger, R. L.; Mucic, R. C.; Storhoff, J. J. *Nature* **1996**, *382*, 607. (c) Sadasivan, S.; Dujardin, E.; Li, M.; Johnson, C. J.; Mann, S. *Small* **2005**, *1*, 103.
(22) (a) Ryadnov, M. G.; Ceyhan, B.; Niemeyer, C. M.; Woolfson, D. N. *J. Am. Chem. Soc.* **2003**, *125*, 9388. (b) Li, M.; Dujardin, E.; Mann, S. *Chem. Commun.* **2005**, 4952.
(23) (a) Connollv, S.; Fitzmaurice, D. *Adv. Mater.* **1999**, *11*, 1202. (b) Li, M.; Wong, K. K. W.; Mann, S. *Chem. Mater.* **1999**, *11*, 23.
(24) Shenton, W.; Davis, S. A.; Mann, S. *Adv. Mater.* **1999**, *11*, 449.
(25) Luna, A.; Amekraz, B.; Tortajada, J.; Morizur, J. P.; Alcami, M.; Mo, M.; Yanez, M. *J. Am. Chem. Soc.* **1998**, *120*, 5411.
(26) (a) Zhang, Z.; Sun, H.; Shao, X.; Li, D.; Yu, H.; Han, M. *Adv. Mater.* **2005**, *17*, 42. (b) Zhang, Z.; Shao, X.; Yu, H.; Wang, Y.; Han, M. *Chem. Mater.* **2005**, *17*, 332.
(27) Weiner, S.; Albeck, S.; Addadi, L. *Chem. Eur. J.* **1996**, *2*, 278.
(28) (a) Weiner, S.; Addadi, L. *J. Mater. Chem.* **1997**, *7*, 689. (b) Mann, S. *J. Chem. Soc., Dalton Trans.* **1997**, 3953. (c) Bigi, A.; Boanini, E.; Walssh, D.; Mann, S. *Angew. Chem., Int. Ed.* **2002**, *41*, 2163.
(29) Labrenz, M.; Druschel, G. K.; Ebert, T. T.; Gilbert, B.; Welch, S. A.; Kemner, K. M.; Logan, G. A.; Summons, R. E.; Stasio, G. D.; Bond, P. L.; Lai, B.; Kelly, S. D.; Banfield, J. F. *Science* **2000**, *290*, 1744.
(30) Zhang, H.; Hussain, I.; Brust, M.; Cooper, A. I. *Adv. Mater.* **2004**, *16*, 27.
(31) Tong, H.; Ma, W.; Wang, L.; Wan, P.; Hu, J.; Cao, L. *Biomaterials* **2004**, *25*, 3923.
(32) Naka, K.; Tanaka, Y.; Chujo, Y. *Langmuir* **2002**, *18*, 3655.
(33) Parker, F. S. *Application of Infrared Spectroscopy in Biochemistry, Biology, and Medicine*; Plenum: New York, 1971.
(34) (a) Gower, L. B.; Odom, D. J. *J. Cryst. Growth* **2000**, *210*, 719. (b) Sethmann, I.; Putnis, A.; Grassmann, O.; Lobmann, P. *Am. Mineral.* **2005**, *90*, 1213.
(35) Penn, R.; L. Banfield, J. F. *Science* **1998**, *281*, 969.
(36) (a) Cölfen, H.; Antonietti, M. *Langmuir* **1998**, *14*, 582. (b) Yu, S. H.; Cölfen, H.; Hartmann, J.; Antonietti, M. *Adv. Funct. Mater.* **2002**, *12*, 541. (c) Yu, S. H.; Cölfen, H.; Tauer, K.; Antonietti, M. *Nat. Mater.* **2005**, *5*, 51. (d) Cölfen, H. *Macromol. Rapid Commun.* **2001**, *22*, 219. (e) Yu, S. H.; Cölfen, H. *J. Mater. Chem.* **2004**, *14*, 2124.
(37) (a) Busch, S.; Dolhaine, H.; DuChesne, A.; Heinz, S.; Hochrein, O.; Laeri, F.; Podebrad, O.; Vietze, U.; Weiland, T.; Kniep, R. *Eur. J. Inorg. Chem.* **1999**, 1643. (b) Kniep R.; Busch, S. *Angew. Chem., Int. Ed.* **1996**, *35*, 2624. (c) Sasaki, N.; Murakami, Y.; Shindo, D.; Sugimoto, T. *J. Colloid Interface Sci.* **1999**, *213*, 121. (d) Sugimoto, T.; Khan, M. M.; Muramatsu, A. *Colloid Interface A* **1993**, *70*, 167. (e) Yu, S. H.; Cölfen, H.; Antonietti, M. *J. Phys. Chem. B* **2003**, *107*, 7396. (f) Cölfen, H.; Qi, L. M. *Chem. Eur. J.* **2001**, *7*, 106.